



RESEARCH LETTER

10.1002/2016GL072398

Key Points:

- On average, large waves occur in the center of wave groups
- Steep waves, which are not necessarily large, tend to be at the front of wave groups
- Most commonly, rogue waves are noticeably larger than the prior and following crests

Correspondence to:

J. Gemmrich,
 gemmrich@uvic.ca

Citation:

Gemmrich, J., and J. Thomson (2017), Observations of the shape and group dynamics of rogue waves, *Geophys. Res. Lett.*, *44*, 1823–1830, doi:10.1002/2016GL072398.

Received 21 DEC 2016

Accepted 27 JAN 2017

Accepted article online 31 JAN 2017

Published online 17 FEB 2017

Observations of the shape and group dynamics of rogue waves

Johannes Gemmrich¹ and Jim Thomson²

¹Department of Physics and Astronomy, University of Victoria, Victoria, British Columbia, Canada, ²Applied Physics Laboratory, University of Washington, Seattle, Washington, USA

Abstract Surface elevation records from two locations in the northeast Pacific are used to examine rogue waves and the relationship to wave groups. Three hundred individual rogue waves with heights greater than 2.2 times the significant wave height are found in analyzing $>2 \times 10^6$ wave groups. In contrast to recent nonlinear modeling results, we do not find that rogue waves occur at the front of wave groups. There is a tendency for steep waves to occur at the front of a group, but these are not the largest waves of the group and do not meet the rogue wave criterion. Rogue waves are most commonly located in the center of the group, but their height ratio to the neighboring crest is greater than in the average wave group. Assessing group dynamics in terms of spectral width suggests that random superposition of nonlinear waves is sufficient to explain the observations of individual rogue waves.

1. Background

Rogue waves are individual waves that are large compared to the surrounding average sea state. They are commonly defined as waves with a trough-to-crest height $H_x \geq 2.2H_s$ (note, some studies use $H_x \geq 2.0H_s$), or a crest height $\eta_x \geq 1.25H_s$, where H_s is the significant wave height [e.g., *Dysthe et al.*, 2008]. Assuming linear theory and a narrowbanded spectrum, the distribution of wave heights is given by the Rayleigh distribution [*Longuet-Higgins*, 1952]. Several related probability distributions for wave heights or crest heights exist for more realistic wave conditions. (For a summary see, e.g., *Gemmrich and Garrett* [2011].) Following these rogue wave definitions, which are purely based on the ratio of the height of an individual wave relative to the background sea state, the likelihood of rogue waves can be calculated from the theoretical distributions. The Rayleigh distribution is generally seen as lower limit, i.e., giving the lowest probabilities for extreme waves, and a rogue wave, $H_x \geq 2.2H_s$, occurs on average every $\approx 1.6 \times 10^4$ waves. Of course, of main interest are rogue waves in high sea states. Mariners sometimes describe rogue waves as a “wall of water,” implying not only a long crest but also a rather stark increase in height compared to the previous crest. Others reported rogue waves to occur in small groups, referred to “three sisters,” with a gradual buildup in height.

The generation of rogue waves in deep water and the absence of currents can be broadly attributed to two possible mechanisms [*Garrett and Gemmrich*, 2009]: (i) the random superposition of linear waves, modified by nonresonant higher-order bound waves [e.g., *Gemmrich and Garrett*, 2011] or (ii) the result of resonant third-order modulational instabilities [e.g., *Janssen*, 2003]. Neither mechanism can be ruled out by the limited observational evidence of the occurrence rate and the maximum height of rogue waves. The modulational instability has been demonstrated in laboratory experiments [*Onorato et al.*, 2004] and evaluated in numerical simulations [see *Toffoli et al.*, 2010]; its relevance for oceanic applications however has been questioned, mainly due to the requirements of narrow spectral bandwidth and narrow directional spreading and the onset of wave breaking prior to the full evolution of the rogue wave. Most studies of rogue waves concentrate on occurrence rates and/or wave heights, and little is known about the shape and persistence of rogue waves [*Baschek and Imai*, 2011; *Christou and Ewans*, 2014; *Romolo and Arena*, 2015].

A recent mathematical study predicts that “large waves tend to move to the front of a wave packet meaning that the locally largest wave is relatively bigger than the wave preceding it” [*Adcock et al.*, 2015]. The authors started from a linear random wavefield and simulated the theoretical nonlinear evolution of the largest waves according to the nonlinear Schroedinger equation [*Trulsen and Dysthe*, 1996]. They also found that the nonlinear evolution does not significantly alter the resulting maximum crest height, but it extends the temporal persistence as well as the width of the extreme crest.

The findings of *Adcock et al.* [2015] on the sudden increase in crest height are related to the concept of “unexpected waves,” i.e., waves that are a factor α times higher than any of the preceding n waves [*Gemmrich and Garrett*, 2008, 2010]. Based on linear simulations, a wave that is at least twice as high ($\alpha = 2$) as any of the preceding $n = 30$ waves occurs on average every 3×10^4 waves, or about twice as often if simulations include the second-order Stokes corrections. Unexpected waves are not necessarily large waves. In fact, only $<20\%$ are rogue waves with $H_x > 2.2H_s$. The likelihood of “unexpected rogue waves,” conditioned on $\eta_x > \xi H_s$, is given in *Fedele* [2016]. *Adcock et al.* [2015] find $\alpha \leq 3$ for the bulk of their simulations but do not specifically consider the length of the quiescent period n , or the amplification factor ξ .

2. Wave Group and Rogue Wave Data Analysis

Observations of the width and persistence of rogue waves would require long-term observations of the sea surface at a spatial coverage of $O(1 \text{ km}^2)$ and a sampling rate of a few seconds, preferable in the open ocean. Such data have been obtained with marine radar or stereographic video [*Lund et al.*, 2014; *Benetazzo et al.*, 2015], but record lengths are usually too short for a statistical analysis of extreme events. However, the shape of wave groups and the relative height change between successive crests can be studied from fixed location time series, which are readily available. Here we use two records from the North Pacific: an open ocean data set at Station P (50°N , 145°W), obtained with a Datawell waverider buoy from June 2010 to January 2014, with $0.8 \text{ m} < H_s < 11.7 \text{ m}$. The other data set, Hecate Strait, was recorded July 2014 to June 2015 with a moored pressure recorder 16 m below the mean surface in 134 m water depth. The location ($52^\circ 49.24''\text{N}$, $129^\circ 50.75''\text{W}$) is in a wide coastal strait subject to frequent storms, and in this record $0.2 \text{ m} < H_s < 4.5 \text{ m}$. The depth attenuation of pressure fluctuations implies a gradual attenuation of the high-frequency wave components, and therefore, H_s and H_x values are slightly biased low. A reconstruction of the high-frequency components could be done based on higher-order corrections. However, the result would only reflect the applied theory, rather than providing more insight, and is therefore not attempted [*Forristall*, 2000].

There are $\approx 6.1 \times 10^6$ waves in the Station P record, and $\approx 2.5 \times 10^6$ in the Hecate Strait record. The height and time of each crest and trough is extracted from the surface elevation time series $\eta(t)$ using the MATLAB toolbox WAFO [*Brodtkorb et al.*, 2000]. The significant wave height H_s is a statistical descriptor of the characteristic wave height and depends on the actual record length [*Gemmrich et al.*, 2016] and the calculation method. Here we base H_s on 40 min data segments and calculate it as the average of the one third highest waves, $H_{1/3}$, as well as the commonly used quantity $H_{\text{std}} = 4\sigma(\eta)$ based on the standard deviation σ . In narrowbanded wavefields $H_s = H_{\text{std}}$. At both locations we find $H_{\text{std}} > H_{1/3}$, indicative of broadband spectra. The number of “rogue waves” at Station P are (209, 33) based on the wave height condition $H_x > 2.2H_s$ and (363, 68) if based on crest height $\eta_x > 1.25H_s$, and $H_s = H_{1/3}$ and $H_s = H_{\text{std}}$, respectively. The corresponding numbers of rogue waves in the Hecate Strait record are (91, 29) and (44, 11). For a linear, narrowbanded wavefield the distribution of wave heights and crest heights are given by Rayleigh distributions, and the exceedance probabilities are $P(H/H_s > z) = \exp(-2z^2)$ and $P(\eta/\eta_s > z) = \exp(-8z^2)$ [*Longuet-Higgins*, 1952], both yielding a straight line on a plot $\ln(-\ln(P))$ versus $\ln(z)$ [see, e.g., *Gemmrich and Garrett*, 2011]. The wave height exceedance data from both records are above the Rayleigh curve, i.e., are less frequent than the Rayleigh prediction, indicating a broadband wavefield, whereas the crest height data are below the Rayleigh line, i.e., are more frequent, indicating a deviation from a purely linear wavefield (Figure 1). Reasonable agreement can be achieved with empirical crest height distributions allowing for nonlinear effects, [e.g., *Kriebel and Dawson*, 1993]. Interestingly, the Station P data show a pronounced curvature of the exceedance probability plot at large values of z which has been observed previously and is not consistent with standard models of wave and crest height distributions [*Dysthe et al.*, 2008; *Gemmrich and Garrett*, 2011]. This curvature suggests a dramatic increase in the occurrence of rare large waves and might be associated with a pronounced role of higher-order bound waves [*Gemmrich and Garrett*, 2011].

The wavefields at both locations are clearly not narrowbanded, and in the following analysis the surface elevation records are normalized by the significant wave height, $\tilde{\eta}(t) = \eta(t)/H_s(t)$, where $H_s = H_{1/3}$. Individual wave groups are identified by local minima \mathcal{H}_{min} of the wave envelope \mathcal{H} , with $\mathcal{H}_{\text{min}} < 0.25H_s$. To calculate the envelope \mathcal{H} , we use complex demodulation, centered at the mean dominant wave frequency ω_p and a filter cutoff of $0.4\omega_p$. For each group we identify each individual crest and its normalized height $\tilde{\eta}_c = \eta_c/H_s$. In particular, the locally largest crest including its position i_x and height $\tilde{\eta}_x = \eta_x/H_s$ are recorded. The data set at Station P consists of $\approx 1.4 \times 10^6$ wave groups, the Hecate Strait record of $\approx 4.5 \times 10^5$.

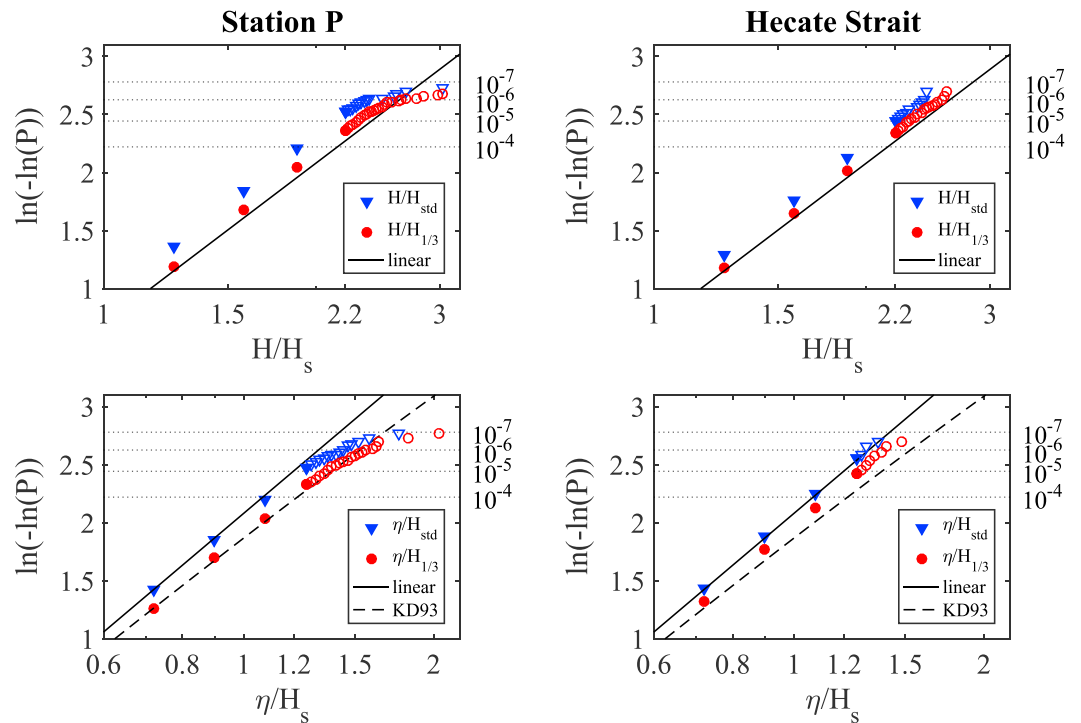


Figure 1. Exceedance probabilities for (top row) wave heights and (bottom row) crest heights for (left column) Station P and (right column) Hecate Strait. The filled symbols are representative points, whereas the open symbols represent individual records. The solid lines show the Rayleigh distributions and the dashed lines the distribution suggested by Kriebel and Dawson [1993] with $R = 0.25$. Values of the exceedance probability P are shown on the right-hand axis.

3. Asymmetry of Wave Groups

A key finding of the simulations by Adcock *et al.* [2015] is the asymmetry of the groups that contain the largest waves. A strong asymmetry of the wave envelope has been reported from wave tank observations [Shemer *et al.*, 2001], and nonlinear simulations of the Euler equation [Slunyaev, 2015], but to our knowledge not in open ocean data.

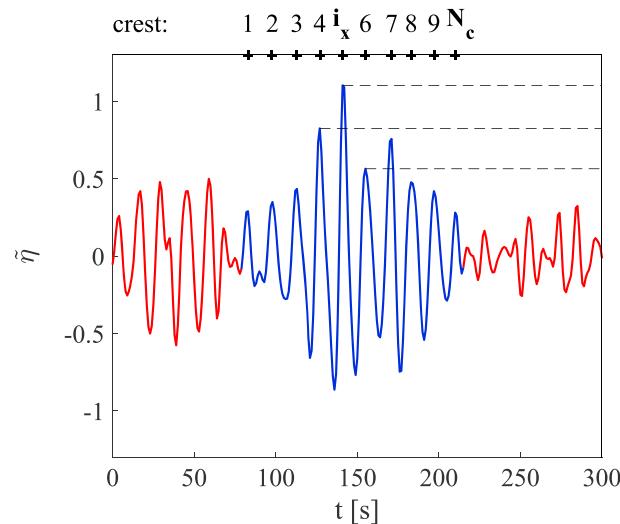


Figure 2. Normalized surface elevation record showing definitions of wave group parameters. (Hecate Strait 14 July 2014, 16:57 UTC). Blue line: wave group with group asymmetry $\zeta = 0.44$ (equation (1)), and step sizes $\sigma_1 = 0.2518$, $\sigma_2 = 0.4882$ (equation (2)).

The degree of group asymmetry can be assessed by the relative position of the largest crest within a wave group:

$$\zeta = \frac{i_x - 1}{N_c - 1}, \quad (1)$$

where N_c is the number of crests within the group and i_x is the index of the largest crest ($1 \leq i_x \leq N_c$) and $0 \leq \zeta < 0.5$ indicates that the largest crest occurs toward the front of the group. For example, the wave group highlighted in Figure 2 consists of $N_c = 10$ crests with the fourth crest being the largest, $\zeta = 0.444$. In both data sets the largest crests occur at any position within the wave groups, but symmetric groups, $0.34 < \zeta < 0.66$, are slightly more common than groups with the maximum near the front ($\zeta < 0.34$) or near the rear ($\zeta > 0.66$) (Figures 3a and 3e). Limiting the analysis to rogue waves,

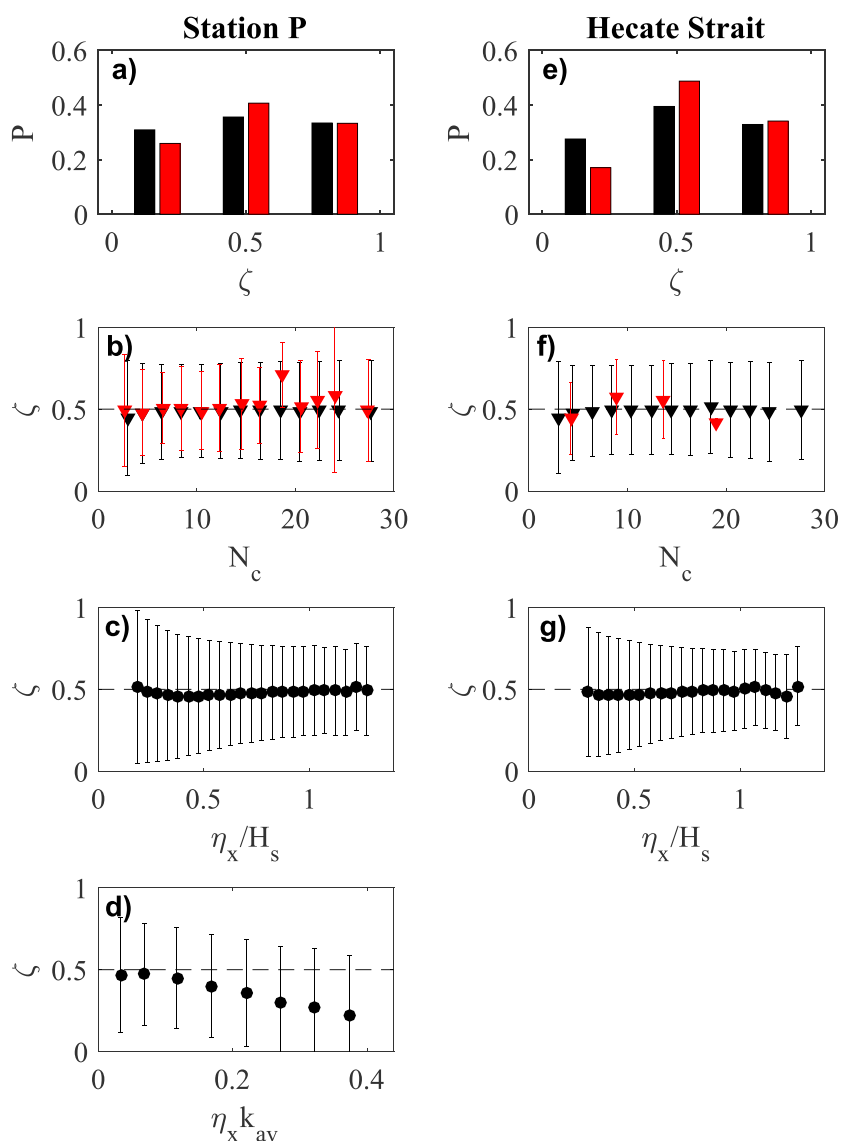


Figure 3. Wave group asymmetry, given as the relative position of the largest crest within a wave group ζ (equation (1)). (a–d) Station P. (e–g) Hecate Strait. Distributions of ζ (Figures 3a and 3e) and ζ as function of the group length N_c (Figures 3b and 3f), the normalized crest height (Figures 3c and 3g), and as function of wave steepness (Figure 3d). Error bars indicate the data spread of ± 1 standard deviation. Black circles indicate all data, black triangles and black bars indicate groups with $\eta_x < 1.25H_s$, and red triangles and red bars indicate groups with $\eta_x \geq 1.25H_s$.

the predominance of symmetric wave groups becomes more prominent. In fact, rogue waves occurring in the first third of a group is the least common case (Figures 3a and 3e).

The most common cases are nearly symmetric wave groups. To propagate the largest crest toward the front of the group would require a certain time for the group to stay coherent, i.e., a minimum group length N_c . This minimum period is expected to decrease with increasing wave nonlinearity. Thus, one could expect a dependence of the relative crest position on the group length, the relative wave height, and the wave steepness. On average the largest crest position is in the middle of the group, $\bar{\zeta} \approx 0.5$, independent of the group length (Figures 3b and 3f) and the normalized height of the crest (Figures 3c and 3g). Furthermore, smaller crests span the entire range of positions within the group, but large waves, including rogue waves, are concentrated near the center (Figures 3c and 3g). This is consistent with the complex growth behavior of nonbreaking crests within wave groups, where faster waves, moving toward the front of the group, are associated with decreasing height [Banner *et al.*, 2014].

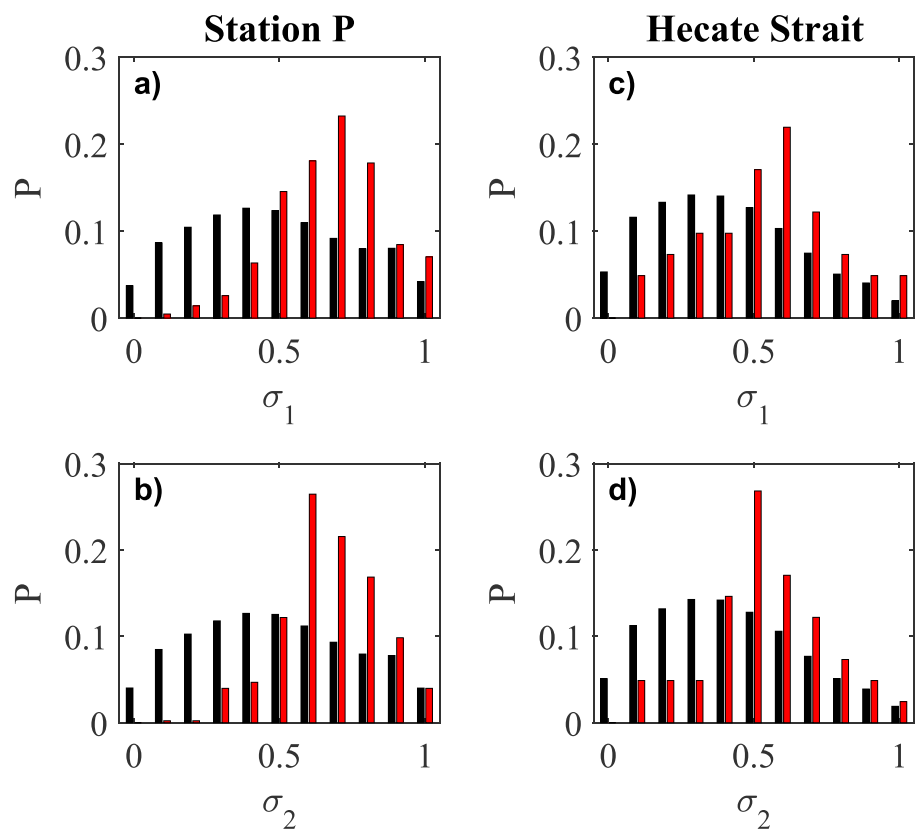


Figure 4. (a and c) Step size σ_1 (equation (2)) relative to prior crest. (b and d) Step size σ_2 (equation (2)) relative to following crest. For groups with $\eta_x < 1.25H_s$ (black) and groups with rogue waves, $\eta_x \geq 1.25H_s$ (red). Station P (Figures 4a and 4b) and Hecate Strait (Figures 4c and 4d).

The nonlinearity of the largest wave depends on its steepness $\eta_x k_x$, rather than solely its height. Here we take $\eta_x k_{av}$ as a measure of the characteristic wave group steepness, where k_{av} is the average wave number of all waves within the group. This is a robust measure but, being based on the linear dispersion relation, likely underestimates the true wave steepness. There is a clear trend of wave groups becoming asymmetric and the largest waves occurring closer to the beginning of the group with increasing group steepness (Figure 3d), qualitatively consistent with the modeling results of Adcock *et al.* [2015]. Note that the surface elevation inferred from the pressure sensor is not suitable for a meaningful analysis of wave steepness and spectral shape.

4. Unexpectedness of Large Waves

The notion of a large wave being “wall like” implies a long crest length and a wave being significantly larger than the previous crest. Only the latter property may be addressed from point observations, and here it is measured by the relative step size of the largest crest height η_x in relation to the prior crest η_1 , or the following crest η_2 (Figure 2):

$$\sigma_1 = \frac{\eta_x - \eta_1}{\eta_x}, \quad \sigma_2 = \frac{\eta_x - \eta_2}{\eta_x}. \quad (2)$$

Gemmrich and Garrett [2008] introduced the term “unexpected wave” for waves at least twice as high as any of the preceding $n_a = 30$ waves. To describe a wave crest as a “wall of water” is a subjective definition, at best. Here we suggest $0.5 \ll \sigma_1 \leq 1.0$ as a criterion for a wave being wall like but do not impose any condition on the minimum length n of the quiescent period.

In most cases the highest crest within a group follows a gradual buildup and wave heights gradually decline afterward (Figure 4). However, rogue waves ($\bar{\eta}_x \geq 1.25$) tend to be noticeable larger than the neighboring waves, and the most common relative step size is $\sigma_{1,2} \approx 0.6$ to 0.7 for the Station P data, and somewhat less for the coastal region.

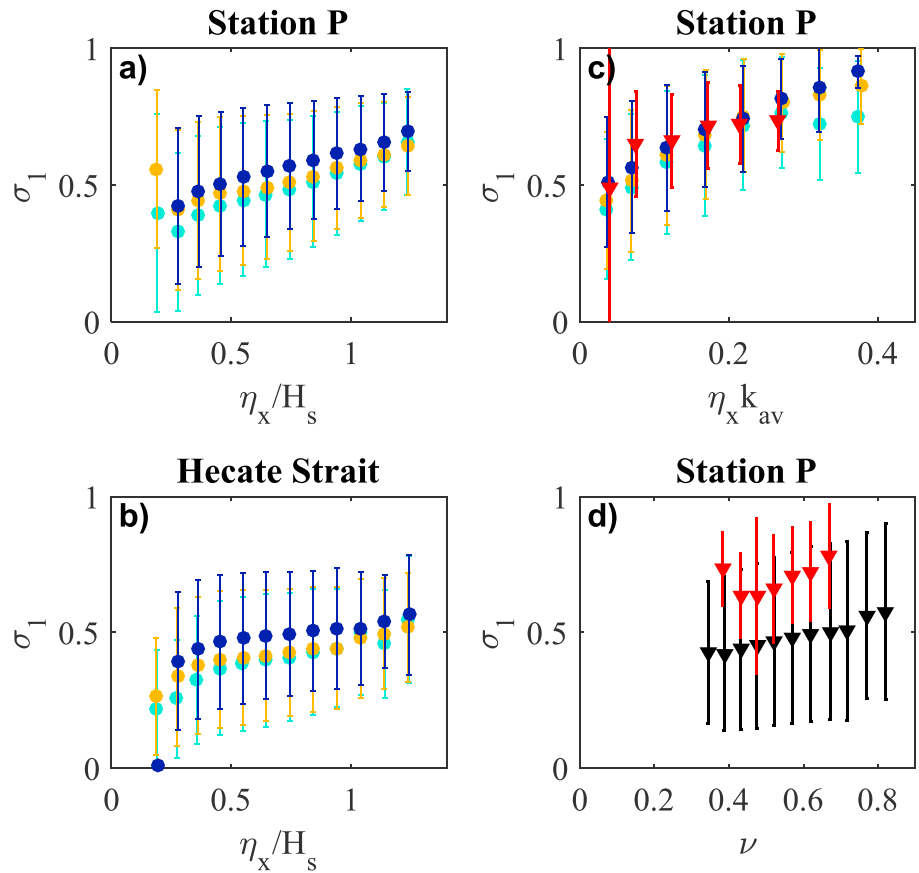


Figure 5. Step size σ_1 of the largest crest within a wave group relative to prior crest (equation (2)), as function of the normalized crest height, for (a) Station P and (b) Hecate Strait, and for Station P only as function of (c) wave steepness and (d) spectral band width ν . Error bars mark the data spread of ± 1 standard deviation. Colored circles indicate the position of the largest crest within the group (blue: front, yellow: center, and cyan: rear). Black triangles indicate groups with $\eta_x < 1.25H_s$, and red triangles $\eta_x \geq 1.25H_s$.

Perhaps not surprisingly, the relative step size σ_1 increases with increasing relative height $\tilde{\eta}_x$ of the locally largest crest (Figures 5a and 5b). Thus, wave groups do not scale with the maximum crest height, but smaller crests occur amongst similar crest heights, resulting in a relatively flat wave envelope, whereas the larger crests tend to be significantly larger than the neighboring crests and the wave envelope is more peaked. Given the same relative crest height, the step size is about 9% higher for crests occurring near the front of the group, $\zeta < 0.33$, compared to groups with $\zeta > 0.33$. The largest average step size is 0.69 and is associated with the rare cases of rogue waves near the beginning of a wave group ($\tilde{\eta}_x \geq 1.25$, $\zeta < 0.33$).

The characteristic group steepness $\eta_x k_{av}$ has the strongest impact on the step size σ_1 (Figure 5c). Near the front of the groups, we find an average step size $\sigma_1 \approx 0.5$ for $\eta_x k_{av} \leq 0.05$, increasing to $\sigma_1 = 0.87$ at the steepest waves, $\eta_x k_{av} > 0.35$. If the largest crest occurs in the middle or toward the end of a group, the average step size is about 8% less than for waves of the same steepness, but occurring near the front of the group. Rogue waves follow a similar dependence of step size on wave group steepness, but in this data set, rogue waves are by far not the steepest locally largest waves and $\eta_x k_{av} < 0.28$ (Figure 5c).

The strength of nonlinear focusing also depends on the spectral bandwidth, besides the wave steepness [Janssen, 2003]. Wave groups in sea states with a narrow spectral band stay coherent for longer periods than in a broadband spectrum. This allows for nonlinear instabilities, like the modulational instability or Benjamin-Feir instability, to be more effective. A common, low-order measure of the spectral width is as follows:

$$\nu = \left[\frac{m_0 m_2}{m_1^2} - 1 \right]^{1/2}, \tag{3}$$

where $m_n = \int \omega^n S(\omega) d\omega$ is the n th moment of the surface elevation spectrum $S(\omega)$. Larger values of ν imply a more broadband spectrum. Typical values for wave conditions during a storm are $\nu \approx 0.3$ to 0.5 [Massel, 2013]. At Station P the bandwidth parameter, calculated from 30 min records, ranges from $\nu = 0.35$ to 0.85 , and the relative step size σ_1 increases, on average, from $\sigma = 0.43$ to 0.57 (Figure 5d). In a broader spectrum there is a greater likelihood of a wave crest being preceded by a much smaller crest, than in a narrowbanded spectrum. Thus, the increase in step size for broader spectra may not be due to an increased height of the largest waves, but rather the more variable sequence of crest heights. In fact, in this data set rogue waves occur at intermediate spectral bandwidth $0.43 < \nu < 0.57$, and there is no correlation between step size and spectral bandwidth in the rogue wave subset (Figure 5d).

The ratio between the wave steepness and the bandwidth defines the so-called Benjamin-Feir Index (BFI) as a measure of nonlinear focusing. Larger BFI values indicate a greater probability of rogue wave occurrences [Onorato et al., 2001; Janssen, 2003] and therefore should also affect the shape of the wave envelope. In the data set at hand, neither the relative position ζ nor the step size σ_1 depends systematically on BFI (not shown). Furthermore, the subset of rogue waves, $\tilde{\eta}_x \geq 1.25$, spans only the lowest third of the BFI values. Thus, Benjamin-Feir instability is likely not a prominent mechanism causing rogue waves in these data sets.

5. Conclusions

Based on a large open ocean data set of $>10^6$ wave groups, there is no evidence of asymmetric wave envelopes for large waves, contrary to the result of recent numerical simulations [Adcock et al., 2015]. As pointed out by an anonymous reviewer, asymmetric wave groups might be the consequence of symmetric initial conditions in numerical simulations and wave tank experiments [Lo and Mei, 1985]. Most commonly, the locally largest crest is about twice as high as its predecessor. However, in the case of rogue waves, defined as $\tilde{\eta}_x \geq 1.25$, the preceding crests reach only 20% to 40% of the rogue crest height, contrary to the notion of a gradual buildup, which mariners sometime label “three sisters.” The asymmetry of wave groups and the crest height increases relative to the predecessor, both are positively correlated with the wave steepness. However, rogue waves are not necessarily steep and tend to occur in the middle of the wave group. Since there is also a positive correlation of the spectral bandwidth and the step size, and no significant correlation with the group asymmetry, we expect that nonlinear modulational focusing does not play a noticeable role in the formation of isolated large waves [see also Trulsen et al., 2015; Fedele et al., 2016]. Linear superposition of higher order Stokes waves seems to be a sufficient mechanism that can explain the existence of unexpected, wall-like rogue waves, as well as the observed occurrence rates of rogue waves [Gemrich and Garrett, 2008, 2011].

Acknowledgments

Discussions with Chris Garrett (University of Victoria) helped to shape this work. We thank the reviewers for their constructive comments. The wave data for Hecate Strait were provided by David Spear (Fisheries and Oceans Canada). The wave observations at Station P are maintained by APL-UW and are available via the Coastal Data Information Program, CDIP station 166 (cdip.ucsd.edu).

References

- Adcock, T. A. A., P. H. Taylor, and S. Draper (2015), Nonlinear dynamics of wave-groups in random seas: Unexpected walls of water in the open ocean, *Proc. R. Soc. A*, *471*, 20150660, doi:10.1098/rspa.2015.0660.
- Banner, M., X. Barthelemy, F. Fedele, M. Allis, A. Benetazzo, F. Dias, and W. L. Peirson (2014), Linking reduced breaking crest speeds to unsteady nonlinear water wave group behavior, *Phys. Rev. Lett.*, *112*, 114502, doi:10.1103/PhysRevLett.112.114502.
- Baschek, B., and J. Imai (2011), Rogue wave observations off the US West Coast, *Oceanography*, *24*, 158–165.
- Benetazzo, A., F. Barbariol, F. Bergamasco, A. Torsello, S. Carniel, and M. Sclavo (2015), Observation of extreme sea waves in a space–time ensemble, *J. Phys. Oceanogr.*, *45*(9), 2261–2275, doi:10.1175/JPO-D-15-0017.1.
- Brodtkorb, P., P. Johannesson, G. Lindgren, I. Rychlik, J. Rydén, and E. Sjö (2000), WAFO—A MATLAB toolbox for the analysis of random waves and loads. paper presented at 10th International Offshore and Polar Engineering Conference, ISOPE, vol. 3, pp. 343–350, Seattle, Wash., 28 May–2 Jun.
- Christou, M., and K. Ewans (2014), Field measurements of rogue water waves, *J. Phys. Oceanogr.*, *44*(9), 2317–2335, doi:10.1175/JPO-D-13-0199.1.
- Dysthe, K., H. E. Krogstad, and P. Müller (2008), Oceanic rogue waves, *Annu. Rev. Fluid Mech.*, *40*, 287–310.
- Fedele, F. (2016), Are rogue waves really unexpected, *J. Phys. Oceanogr.*, *46*, 1495–1508.
- Fedele, F., J. Brennan, S. Ponce de León, J. Dudley, and F. Dias (2016), Real world ocean rogue waves explained without the modulational instability, *Sci. Rep.*, *6*, 27715, 1–11.
- Forristall, G. Z. (2000), Wave crest distributions: Observations and second-order theory, *J. Phys. Oceanogr.*, *30*(8), 1931–1943.
- Garrett, C., and J. Gemrich (2009), Rogue waves, *Phys. Today*, *62*(6), 62–63.
- Gemrich, J., and C. Garrett (2008), Unexpected waves, *J. Phys. Oceanogr.*, *38*(10), 2330–2336.
- Gemrich, J., and C. Garrett (2010), Unexpected waves: Intermediate depth simulations and comparison with observations, *Ocean Eng.*, *37*, 262–267.
- Gemrich, J., and C. Garrett (2011), Dynamical and statistical explanations of observed occurrence rates of rogue waves, *Nat. Hazards Earth Syst. Sci.*, *11*, 1437–1446, doi:10.5194/nhess-11-1437-2011.
- Gemrich, J., J. Thomson, W. E. Rogers, A. Pleskachevsky, and S. Lehner (2016), Spatial characteristics of ocean surface waves, *Ocean Dyn.*, *66*, 1025–1035, doi:10.1007/s10236-016-0967-6.
- Janssen, P. A. E. M. (2003), Nonlinear four-wave interactions and freak waves, *J. Phys. Oceanogr.*, *33*, 863–884.
- Kriebel, D. L., and T. H. Dawson (1993), Nonlinear effects on water waves in random seas, *J. Offshore Mech. Arct. Eng.*, *113*, 142–147.

- Lo, E., and C. Mei (1985), A numerical study of water-wave modulation based on a higher-order nonlinear Schrodinger equation, *J. Fluid Mech.*, *150*, 395–416.
- Longuet-Higgins, M. S. (1952), On the statistical distribution of the heights of sea waves, *J. Mar. Res.*, *11*(3), 245–266.
- Lund, B., C. O. Collins, H. C. Graber, E. Terrill, and T. H. Herbers (2014), Marine radar ocean wave retrieval's dependency on range and azimuth, *Ocean Dyn.*, *64*, 999–1018.
- Massel, S. R. (2013), *Ocean Surface Waves: Their Physics and Prediction*, 2nd ed., World Sci., Hackensack, N. J.
- Onorato, M., A. R. Osborne, M. Serio, and S. Bertone (2001), Freak waves in random oceanic sea states, *Phys. Rev. Lett.*, *86*, 5831–5834.
- Onorato, M., A. R. Osborne, M. Serio, L. Cavaleri, C. Brandini, and C. T. Stansberg (2004), Observation of strongly non-Gaussian statistics for random sea surface gravity waves in wave flume experiments, *Phys. Rev. E*, *70*, 067302, doi:10.1103/PhysRevE.70.067302.
- Romolo, A., and F. Arena (2015), On Adler space-time extremes during ocean storms, *J. Geophys. Res. Oceans*, *120*, 3022–3042, doi:10.1002/2015JC010749.
- Shemer, L., H. Jiao, E. Kit, and Y. Agnon (2001), Evolution of a nonlinear wave field along a tank: Experiments and numerical simulations based on the spatial Zakharov equation, *J. Fluid Mech.*, *427*, 107–129.
- Slunyaev, A. (2015), On the wave group asymmetry caused by nonlinear evolution. Geophysical Research Abstracts EGU2015-7079 presented at 2015 General Assembly, EGU, Vienna, 12–17 Apr.
- Toffoli, A., O. Gramstad, K. Trulsen, J. Monbaliu, E. Bitner-Gregersen, and M. Onorato (2010), Evolution of weakly nonlinear random directional waves: Laboratory experiments and numerical simulations, *J. Fluid Mech.*, *664*, 313–336.
- Trulsen, K., and K. Dysthe (1996), A modified nonlinear Schroedinger equation for broader bandwidth gravity waves on deep water, *Wave Motion*, *24*, 281–289.
- Trulsen, K., J. C. Nieto Borge, O. Gramstad, L. Aouf, and J.-M. Lefèvre (2015), Crossing sea state and rogue wave probability during the Prestige accident, *J. Geophys. Res.*, *120*(10), 7113–7136, doi:10.1002/2015JC011161.